Chapter 7

Coating Technology of Nuclear Fuel Kernels: A Multiscale View

Malin Liu

Additional information is available at the end of the chapter

http://dx.doi.org/10.5772/55651

1. Introduction

The coating technology of nuclear fuel kernels (NFKs) is an important part of the nuclear safety research. Now there are many new designs of nuclear reactor which based on the coated fuel particles. Among them, high temperature gas-cooled reactor (HTGR) is one of the Gen-IV reactors and has a bright future in the electricity and hydrogen production because of its superior characteristics.

The inherent safety characteristics of HTGR have been paid more attention among many nuclear reactors in the nuclear renaissance, even more adequately after the Fukushima nuclear accident. The first security assurance is the HTGR nuclear fuel element based on the coated fuel particles, so the coating process of nuclear fuel particles is one of the most important key technologies in the research on HTGR. The tristructural-isotropic (TRISO) type coated fuel particle, which has been commonly used in the current HTGR consists of a microspheric UO_2 fuel kernel surrounded by four coated layers: a porous buffer pyrolysis carbon layer (buffer PyC), an inner dense pyrolysis carbon layer (IPyC), a silicon carbide layer (SiC) and an outer dense pyrolysis carbon layer (OPyC), as shown in Fig.1. All coating layers are prepared in the spouted fluidized bed by chemical vapour deposition (CVD) method in different research groups in Germany, USA, South Korea, Japan and China [1-5].

Now, HTR-PM (high-temperature-reactor pebble-bed module), a Chinese 2×250 MWth HTR demonstration plant, is under construction in Weihai City, Shandong Province, PRC. A pilot fuel production line will be built to fabricate 300,000 pebble fuel elements per year, and each pebble fuel element contains about 15000 coated fuel particles, so the higher requirements for mass production of coated fuel particles for fuel elements are put forward. In order to optimize and scale up the coating process of fuel kernels from the lab to the factory, the multiscale study

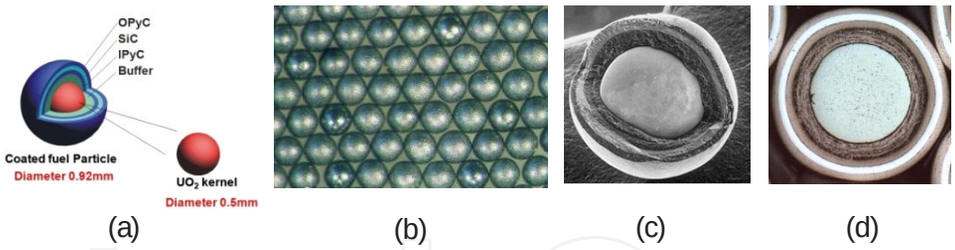

Figure 1. (a) schematic diagram of coating layers, (b) nuclear fuel kernels(~0.5mm), (c) coated fuel particle(~0.92mm), (d) Cross-section of coated fuel particle(~0.92mm)

concept of the coating process was proposed by us in the research process. In this chapter, the details of this multiscale concept will be given based on our scientific research achievements.

2. The coating methods for NFKs

The first layer deposited on the kernels is porous carbon, this is followed by a thin coating of pyrolytic carbon (a very dense form of heat-treated carbon), a layer of silicon carbide and another layer of pyrolytic carbon. Each coating process is performed at a defined temperature and for a defined duration of time. The schematic diagram of the experimental facility is shown in Fig. 2. This experimental facility can be divided into two main parts: the left part is the gas distribution system and the right part is the conical spouted bed coating system. The gas distribution system contains argon, the hydrocarbon gas (ethyne and propene), hydrogen and methyl trichlorosilane (MTS) vapor supply device, flow control system and the gas distribution device. The conical spouted bed coating system contains the spouted bed, the cooling water system, the heating system, the thermal insulation system, the gas airtight device and the temperature control device.

The spherical UO_2 kernel as fuel particles are fluidized by the fluidization gas and coated by the reactive gas in the conical spouted bed coating furnace. The thickness, coating time, coating temperature, reactive and fluidization gas of four coating layers should be determined beforehand in the coating experiments as shown in Table 1.

Coating layer	Thickness /μm	Coating time /min	Reactive+Fluidization gas	Coating temperature / ºC
1. Buffer PyC	95	~2.5	Acetylene+Argon	~1260
2. Inner PyC	40	~12.5	Propylene+ Argon	~1280
3. SiC	35	~150.0	MTS+Hydrogen	~1600
4. Outer PyC	40	~12.0	Propylene+ Argon	~1300

Table 1. Experimental parameters in the coating process of TRISO particle

http://dx.doi.org/10.5772/55651

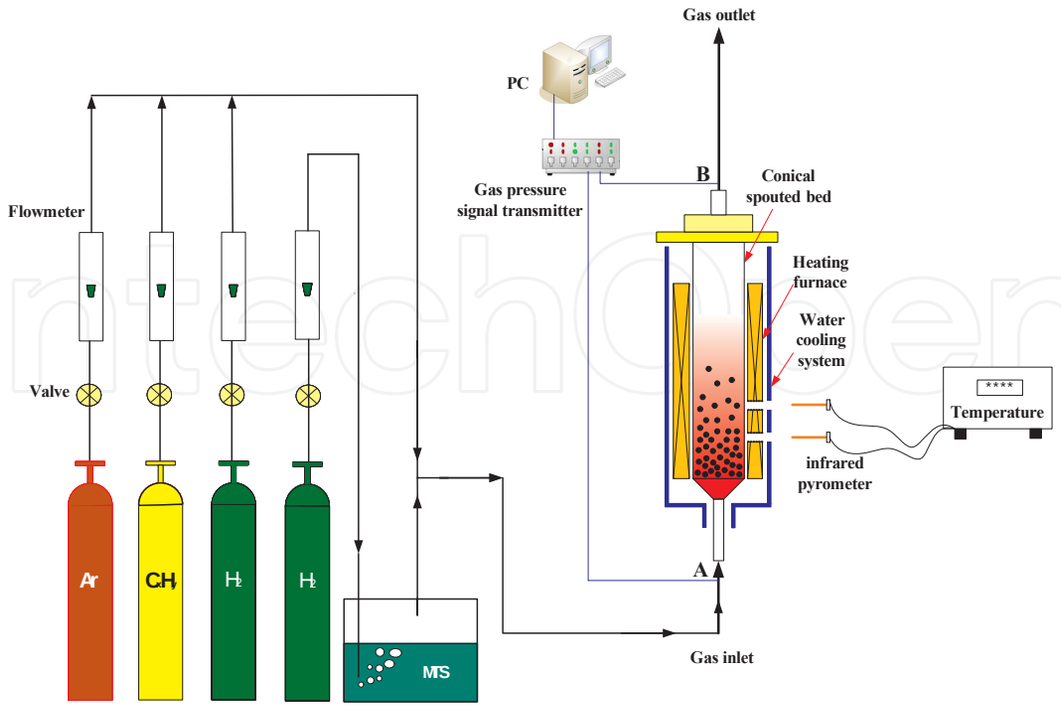

Figure 2. The schematic diagram of the spouted bed coating system

The whole coating process can be described as follows: In the pyrolytic carbon coating process, ethyne and propene as the reactive gas and argon as the fluidization gas are injected into the coating furnace, they are pyrolyzed at the high temperature about 1300ºC and then PyC layers are prepared. The SiC coated layer is prepared by MTS vapor as the reactive gas which is entrained by hydrogen and is pyrolyzed at about 1600 ºC. The integrity and property behavior of the SiC layer of the Tri-isotropic (TRISO) coated particle (CP) for high temperature reactors (HTR) are very important as the SiC layer is the main barrier for gaseous and metallic fission product release.

The fluidized bed chemical vapor deposition (FB-CVD) method is a suitable technique for preparing various kinds of films/layers on the spherical materials by initiating chemical reaction in a gas. FB-CVD has the advantage of large reactor volume to offer sufficient space with uniform mass and heat transfer condition. This technique can be used for other purposes, such as synthesizing carbon nanotube composite photocatalyst ((CNT)/Fe-Ni/TiO_2). Also, some modified method based on FB-CVD, such as plasma-enhanced FB-CVD, has been used to prepare the transparent water-repellent thin films on glass beads in modern surface engineering treatment. So the investigation of FB-CVD method is helpful and important for modern surface treatments.

3. Multiscale analysis

If we only do the coating experiments in the lab scale, it can be done in a very small reactor and the efficiency can be very high, but now the question is the how to develop coating

technology from the lab to the factory? The answer is that we must consider the multiscale study of coating technology of nuclear fuel kernels. The multiscale study of TRISO-coated particle includes three scales: microscale(material microstructure scale, ~nm), mesoscale (mesoscopic scale, paticle size scale, ~mm) and macroscale(reactor size scale, ~m), as shown in Fig. 3.

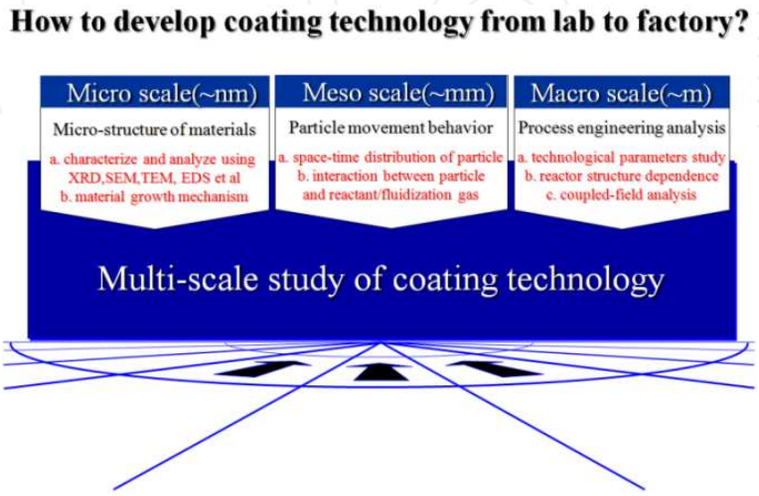

Figure 3. Multiscale study of coating techonolgy of nuclear fuel kernels

The microscale study mainly focused on the micro-structure of materials, including characterize and analyze the coating materials using XRD, SEM, TEM, EDS, et al, and then give the material growth mechanism, using it we can control the material grown as we want. This scale is the basic area of materials research. The deposition mechanism of PyC layer, the microstructure of SiC layer, and the new coating layer, such as ZrC, has been exploited in our studies.

In order to prevent the risk associated with producing particles that do not meet the requirements, a fundamental understanding of the fluidization phenomena occurring in the spouted bed coater is needed. Fluidized-bed CVD is a special technique to coat nuclear fuel particles. To ensure uniform deposits on particles, efficient contact of particles with the reactive gas must be achieved. Knowledge of the solids flow pattern in spouted bed is essential to the design of spouted bed, because the particle trajectories must meet process requirements. So the mesoscale study mainly focused on the particle movement behavior, including the space-time distribution of particles and spout-fluid bed dynamics. The domination factor is the interaction between particle and coating/fluidization gas, which influences the properties of coating materials directly.

The macroscale study mainly focused on the process engineering analysis on the whole coating system, including technological parameters study, reactor structure dependence, coupled-field analysis which include the velocity field, temperature field and material concentration field. An example is the associated research between a reactor-scale pressure changes and the coating process.

http://dx.doi.org/10.5772/55651

3.1. Microscale study

The microscale study mainly focused on characterizing and analyzing the micro-structure of the coating materials by using XRD, SEM, TEM, EDS, et al [6-8]. Based on the examination results, the growth mechanism of coating layers was analyzed and the relation of coating layers microstructure and the deposition technology was established. We have validated the droplet deposition mechanism in the PyC layer [9] and investigated density change reasons in the SiC layer [10]. The relationship between the temperature change and the microstructure of the SiC layer [11], and the new coating layer, such as ZrC, has been exploited.

- The coating process of PyC layer

In the PyC coating process, the ethyne and the propene are injected into a conical fluidized bed coating furnace and pyrolytic carbon is coated on the fuel particle by CVD (chemical vapor deposition). However, pyrolytic carbon has not been fully exploited in the coating process of fuel particles, so a large amount of pyrolytic carbon powder as waste will settle down in the subsequent cyclone separator. The pyrolytic carbon powder is the main solid byproduct generated in the coating process. The pyrolytic carbon powder can be collected as carbon black powder sample, which can be seen as the intermediate products and can be used to study the mechanism of the coating process of the PyC layer.

The microstructure of pyrolytic carbon powder and the PyC layer are investigated using JEM 2010 TEM (JEOL Ltd., Tokyo, Japan). The preparation method of electron microscopy sample is to suspend the PyC layer and carbon black powder in the anhydrous ethanol at first, and then disperse the sample for 15 minutes by adopting the ultrasound method.

The TEM image of the carbon black samples is showed in Fig. 4. It can be found that the pyrolytic carbon black powder is composed of the nano-spherical carbon particles. They are ring-layered nano-structured carbon particles and many layers of carbon atoms arrange tidily in the nano-spherical carbon particles.

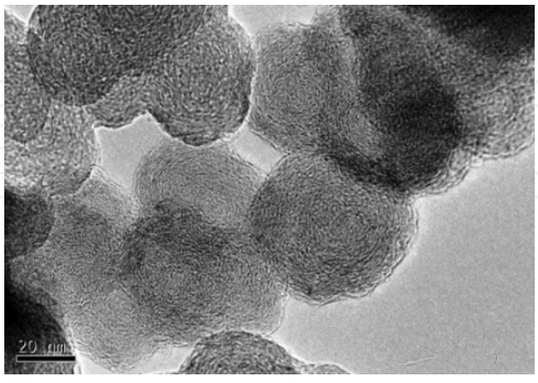

Figure 4. The TEM image of the carbon black sample

The high resolution TEM image in Fig. 5 indicate that the near-ordered structure of nano-spherical carbon particle is mainly characterized by interrupted lattice fringes of 0.34 nm in average. This value is comparable with the (002) d-spacing in graphite 2H and the (003) d-

spacing in graphite 3R. But the carbon atom layer is incomplete here and the structure shows a high defect concentration. The results confirm that the carbon black sample has the layered structure and the near-ordered structure of nano-spherical carbon particle is mainly characterized by lattice fringes of 0.34 nm in average.

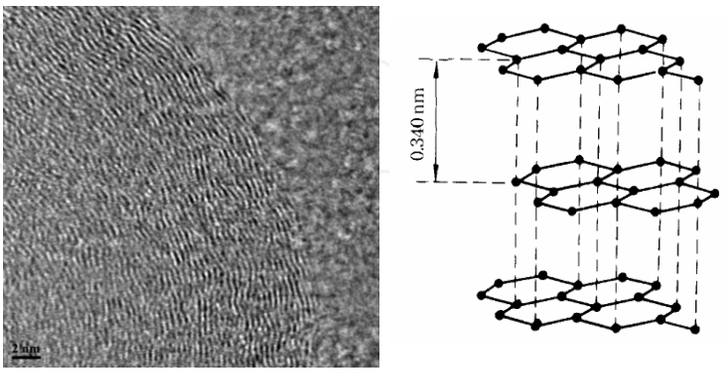

Figure 5. The high resilution TEM image of the carbon black sample

The TEM image of the deposition pyrolytic carbon samples is given in Fig.6. It can be found that agglomeration of carbon nano-particles is much greater. Numerous models have been proposed to describe the carbon deposition mechanism: molecular deposition mechanism, droplet deposition mechanism, surface decomposition theory and so on [12]. The experimental results here have shown that the gas-phase nucleation occur at first and then nano-particles deposit on the surface of fuel particle. The droplet deposition mechanism is suitable to describe the formation of the dense PyC layer in the fuel particle coating process.

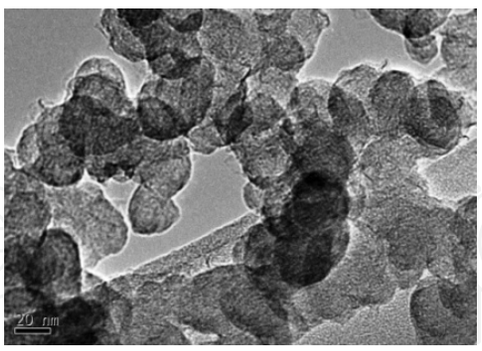

Figure 6. The TEM image of the deposition pyrolytic carbon samples

The schematic diagram of the nano-particles agglomeration is shown in Fig. 7. The nano-particles with the diameter ofabout 50 nm aggregate into the large clusters with the diameter of about 1 μm at first. Then the 1 μm clusters aggregate into the larger cluster with the diameter of 10 μm. Usually, the microstructure of the carbon black powder consists of three grades:(1) the primary particle; (2) the particle aggregates(~1μm), which is the primary structure of the carbon black; (3) the agglomerate(~10μm), which is also known as the secondary structure of

http://dx.doi.org/10.5772/55651

carbon black. The Van der Waals force plays a major role in the agglomerating process of the nano-spherical carbon particle.

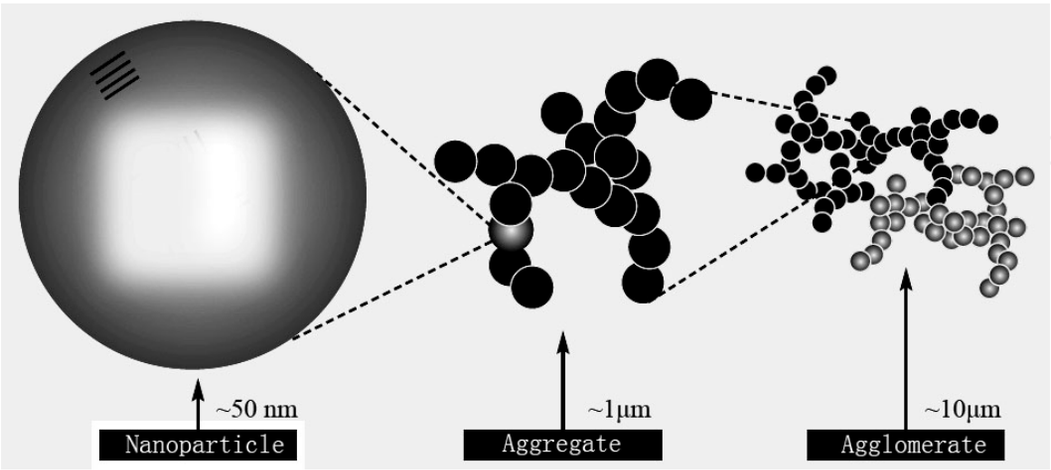

Figure 7. The schematic diagram of the nano-particles agglomeration

From the above discussion, it can be found that the droplet deposition mechanism can be used to explain the formation of the dense PyC layer in the fuel particle coating process. The nano-spherical carbon particles are generated at first, and then deposit on the surface of fuel particle.

- The coating process of SiC layer

The microstructure of the SiC coating layer are invesitgated under different coating temperatures, from 1520-1600ºC. The reasons of density change are discussed based on microstructure analysis. After coating experiments, the coated particle are pressed carefully, until the SiC coated layer are crushed, then the fragments of SiC coated layer are collected carefully, as shown in Fig.8. Prior to characterization analysis, it need to heat the fragments for 10 hours at 800 ºC, to remove the layers of pyrolytic carbon.

Figure 8. Appearances of SiC coating layer after crushing

The XRD analysis results of the cross-section and the surface of the SiC sample produced under different temperatures are almost the same. The peaks located at 36', 60' and 72' are the characteristic peak of the SiC, corresponding to the (111), (220) and (311) crystal face diffraction

of SiC respectively. The peaks located at 41' and 75 'are corresponding to the crystal face (200), (222) diffraction of SiC respectively. The sample has a perfect crystallinity from these characterization results. The pure SiC product is obtained substantially, impurities such as carbon and silicon peaks is not obvious, so the influence of impurities such as carbon can be excluded in the possible reasons of the aforementioned density changes. Thus it can be concluded that SiC without the doped C, Si and other impurities can be prepared in the experimental MTS concentration value, in different temperature from 1 520 ºC to 1 600 ºC.

The Raman spectra of the SiC coating layer obtained under different temperature are shown in Fig. 9. We know that the two characteristic peaks of the β-SiC are the two optical mode (peak): 796cm^{-1}, the TO(transverse optical mode) and 972cm^{-1}, LO (longitudinal optical mode) in the Brillouin zone. As can be seen from Fig.10, The Raman spectral peaks measured experimentally are the peak 1 (796cm^{-1}) and peak 2 (972cm^{-1}), which can be considered as the two characteristic peaks, therefore it can be concluded that β-SiC (3C-SiC) is obtained, and the crystal structure is the zinc-blende structure. There are no characteristic peaks of the α-SiC, it can be determined that the sample are almost pure β-SiC. So β-SiC can be generated in the experimental temperature range from 1520-1600ºC.

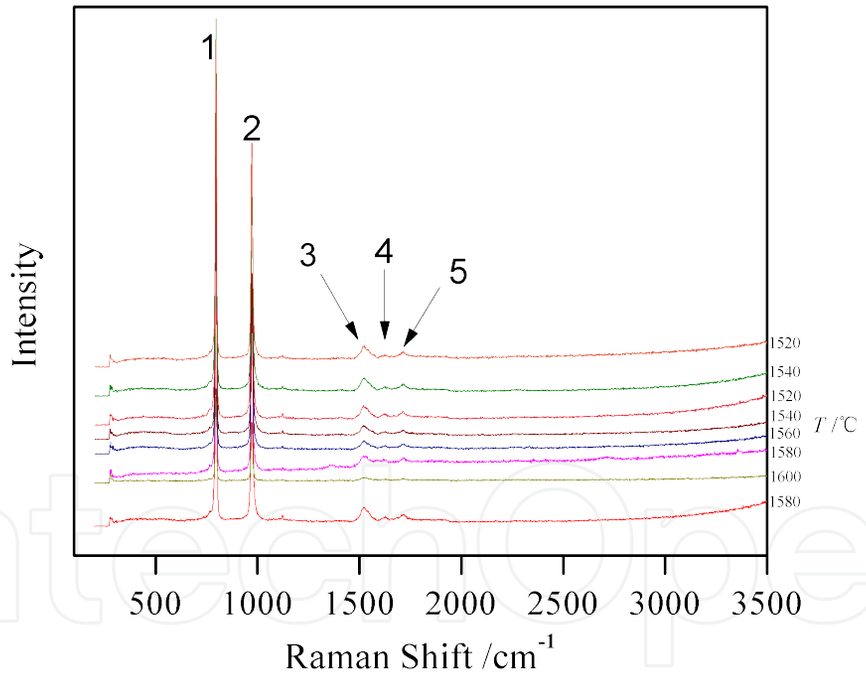

Figure 9. Raman spectrum of SiC coated layer

The secondary Raman peaks of SiC coating layer can also be obtained as: 3#(1 520 cm^{-1}), 4#(1 620 cm^{-1}), 5#(1 720 cm^{-1}) in Fig.9. It is consistant with the literature. From further analysis it can be found that the peak 5 (1 720 cm^{-1}) has a blue shift trend with the decrease in density of the sample, as shown in Fig.10. The reason can be deduced from the literature [13]. The presence of the microscopic pore structure in the sample with low density destroyed the complete lattice structure of SiC crystal, so the lattice vibration frequency increases as a result.

http://dx.doi.org/10.5772/55651

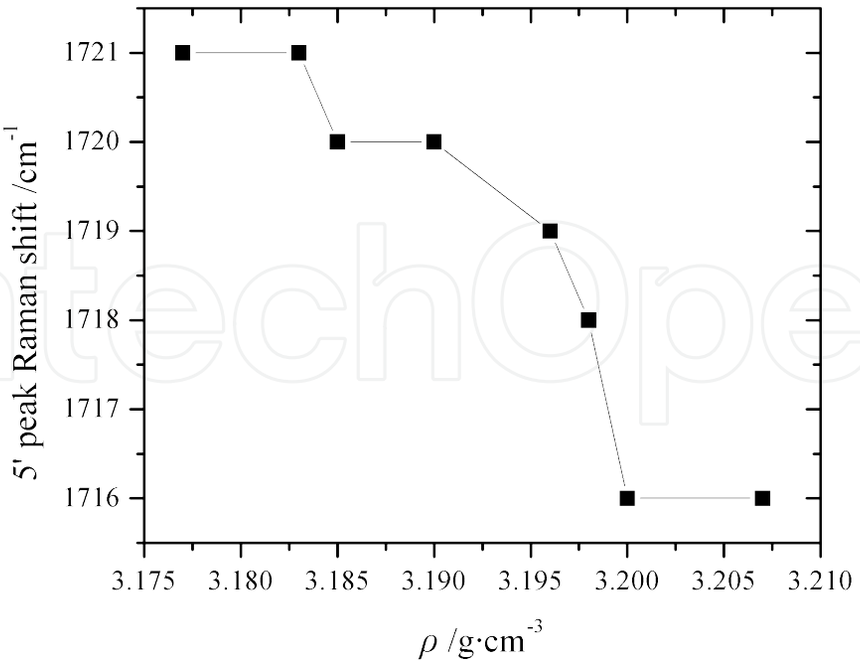

Figure 10. Secondary Raman spectrum of SiC coating layer and temperature *vs* density

The SEM image of the cross-section of the SiC coating layer with low density (ρ=3.177 g/cm^3) are given and the characterization images are shown in Fig. 11. As can be seen from the figure, the coating layer of low density SiC has the the presence of a microporous structure indeed, this is consistent with the results of the Raman spectroscopy. The above results show that the porous structure should be the main reason of which the apparent density of the SiC coating layer is lower than the theoretical value.

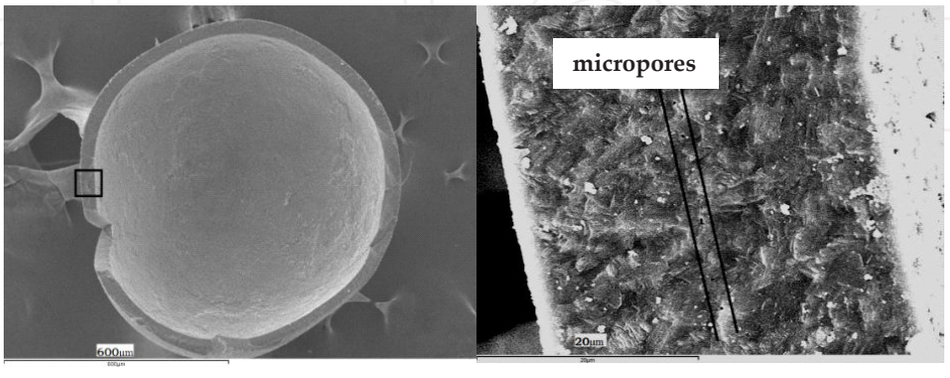

Figure 11. SEM image of shell cross-section of SiC coating layer

The linear distribution of micropores can also be found from Fig. 11, and the linear distribution is parallel to both the inside and outside shell of the SiC coating layer approximately, i.e. the micropores are located at a same deposition surface in the growth process of the SiC coating layer. It can be assumed that during the growth of the SiC coating layer, the SiC layer grows gradually from the inner shell to the outer shell, the temperature or the fluidized state of the particles fluctuate at a certain time point, resulting of interruption occurs in the continuous SiC crystal growth, to produce a linear distribution of micropores. So these micropores are in linear distribution, and parallel to the inner and outer shell approximately. Obviously, these micropores are not conducive to the performance improvement of hindering the fission products, and should be avoided in the actual production process.

To sum up, the pure β-SiC can be prepared in the experimental temperature range from 1520-1600ºC. Microstructure analysis validates that the density change of the SiC coated layer is mainly due to the micropores in the coated layer, not the doped C, Si and other impurities. The linear distribution of the micropores is found, and all micropores are located at the same deposition surface. It can be concluded that the formation of the micropores in the coated layer is closely related to the particle fluidized state, which should be focused on in the mesoscale study.

High temperature oxidation behavior of the SiC coating layer are also investigated. High temperature oxidation experiments were carried out about 10 hours at different temperatures from 800 to 1 600 ºC at air atmosphere. The microstructure and composition were studied using different characterization methods. High-resolution SEM images are given in Fig. 12.

It showed that the oxidation began from the surface and gradually formed a punctate distribution of the oxide. The small crystal structure (~1 μm) of the SiC surface was very clear at 1000 ºC, this crystal structure was disappeared gradually at high temperatures, and oxidized to form oxides of Si in the SiC surface. There was a stacking fault stress due to the different thermal expansion coefficient and elastic modulus of SiC and Si oxides, leading to the gradual formation of cracks around the punctates. With the increasing temperature, the crack further increased the oxidation rate of SiC, finally the formed Si oxides layer fell off from the particles. It can be seen clearly that the layer was peeling when the temperature was increased to 1 400 ºC.

The SEM images of new fracture surface of SiC coating layer after oxidization at 1400 ºC are shown in Fig.13. It can seen obviously that oxidation front-end interface with many micropores are between oxidation layer with the smooth surface and the SiC coating layer with crepe-like texture. It can also be found that the oxidation layer is very thin, only about 1μm, indicating that the oxidation rate is very slow. The oxidation layer was so thin (~1μm) comparing with the original thickness(~35μm) of the SiC coating layer, so the remain SiC coating layer has the same fuction of hindering fission products in the TRISO particles.

http://dx.doi.org/10.5772/55651

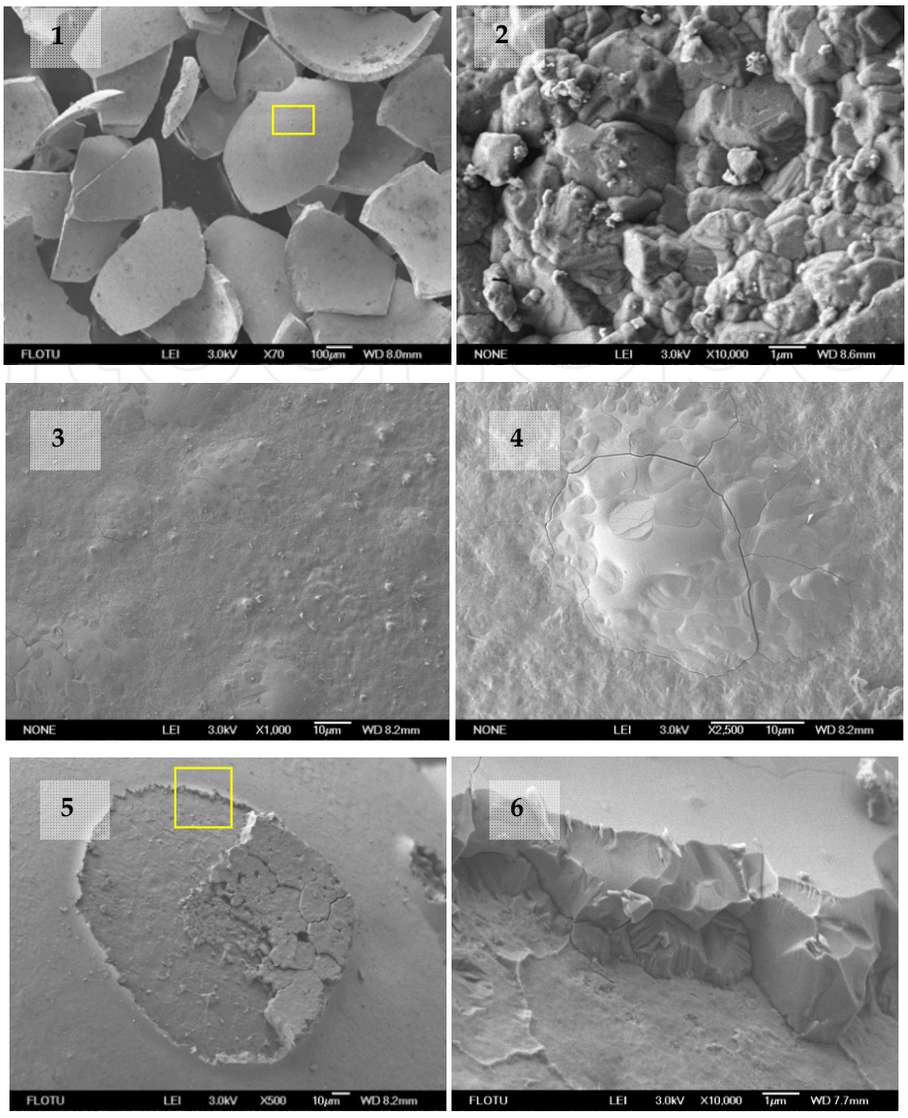

Figure 12. SEM images of SiC coating layer after oxidization at different temperature(1. 1000 ºC, ×70; 2. 1000 ºC, ×10000; 3. 1200 ºC, ×1000; 4. 1300 ºC, ×2500; 5. 1400 ºC, ×500; 6. 1400 ºC, ×10000)

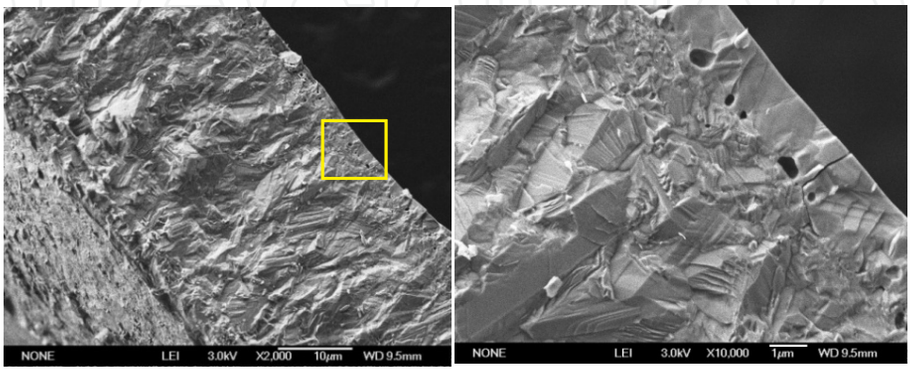

Figure 13. SEM images of SiC fracture surface after oxidization at 1400℃

The XRD characterization results of the SiC coating material after the oxidation test of different temperatures are given in Fig. 14. The SiO_2 peaks gradually appear when the oxidization temperature is more than 1 400 ºC. It showed that there was a growing SiO_2 peaks from 1 400 ºC, indicating that surface oxidation was significant gradually. The relative degree of oxidation is deepened when the temperature rises. The peak is very sharp, which means that SiO_2 is already crystallized. The oxidation behavior found here is consistent with the SEM images above.

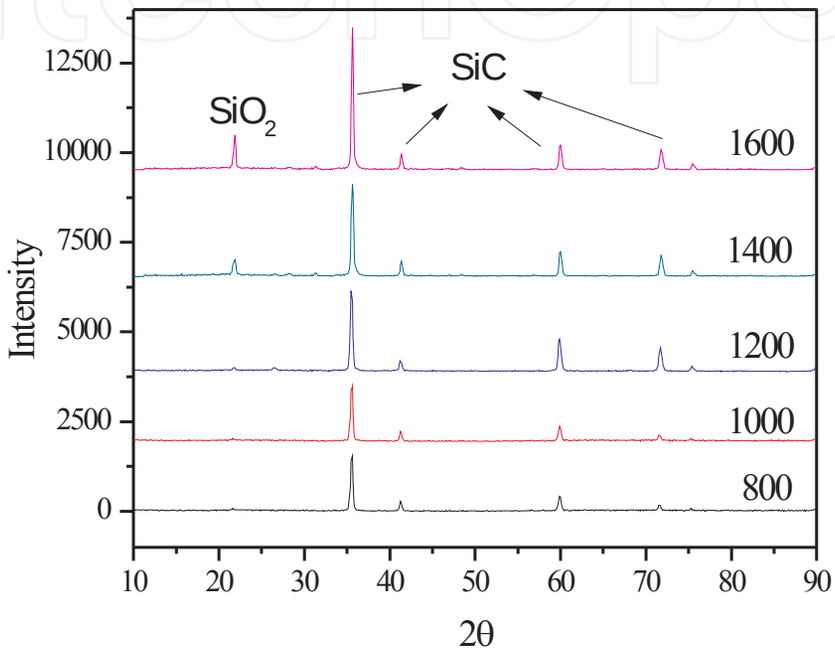

Figure 14. XRD results of the SiC coating layer after oxidization at different temperature

To sum up, the oxidization of the SiC coating layer was not obvious below 1 200 ºC. The oxidization of the SiC coating layer was significant gradually from 1 400 ºC, but the oxidation rate is very slow. So the SiC coating layer has good performance of hindering the fission product, even at the severe air ingress accident in the nuclear power station. The TRISO coated particles can be seen as the first security assurance of the HTGR nuclear fuel element.

3.2. Mesoscale study

The mesoscale study mainly focused on how to improve gas-solid contact efficiency, which based on a fundamental understanding of the fluidization phenomena of high density particles (UO_2, ~10.86g/cm^3) occurring in the spouted bed coater. In our work, the particle movement behaviors including the space-time distribution of particles and spout-fluid bed dynamics based on Euler-Euler simulation were studied [14]. It was found that the specially designed multi-nozzle gas inlet is better than the single-nozzle gas inlet for obtaining a more uniform fluidization, which can disperse the gas to increase the gas-particle contact efficiency. Also we have established the DEM-CFD simulation platform. The spout process was simulated based

on this coupling method. Some key parameters in coating process are proposed and the scale-up technology has been developed. It was emphasized that efficient contact of particles with the reactive gas must be achieved to ensure uniform deposition on particles.

- Euler-Lagrange simulation

The coating layer on the UO_2 fuel kernel surface is prepared by chemical vapor deposition when the gases are injected into the spouted bed coating furnace. One of the major factors to influence coating performance is the contact efficiency between the gas and the solid particles, which is determined by the hydrodynamics in the spouted bed nuclear fuel particle coated furnace. The hydrodynamics of a spouted bed are important from a CVD perspective because they directly determine the magnitude and variability of the concentration and species gradients in the zone where the reactant gases first come into contact with hot particles. It is recommended for the gas distributor to disperse the gas over the full area of the coating chamber to enhance gas-particle contact efficiency. Specifically, the particle flow in spouted bed consists of three distinct regions: a dilute phase core of upward gas-solid flow called the "spout", a surrounding region of downward quasi-static granular flow called the "annulus", and a top area called " fountain" between these aforementioned two regions as shown in Fig. 15.

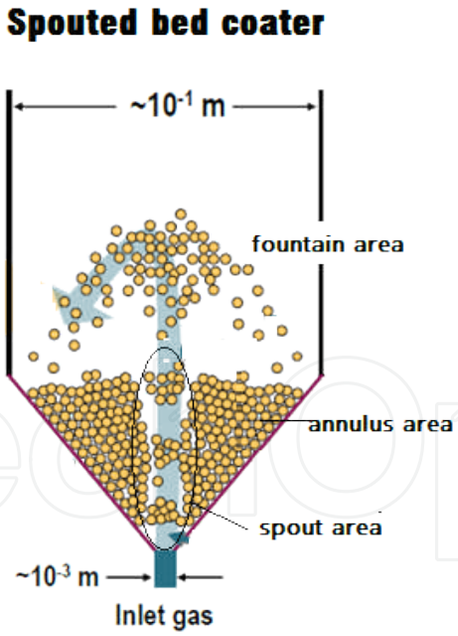

Figure 15. The spout area, annulus area and fountain area in the spouted bed coater

Generally, one particle is flowed up in spout area, and contacted with the reaction gas, coated by the CVD products, and then, falling down into the annulus area, which can not contact with the reaction gas. So the key parameters in coating process are the volume of spout area (V_s), the oscillation cycle period of particle clusters (T_c), the single particle cycle time(T_p) and the

time period of particle in spout area in a particle cycle time(T_s). It is difficult to measure these key parameters in experiments, but it is easy to obtain them in the simulation results.

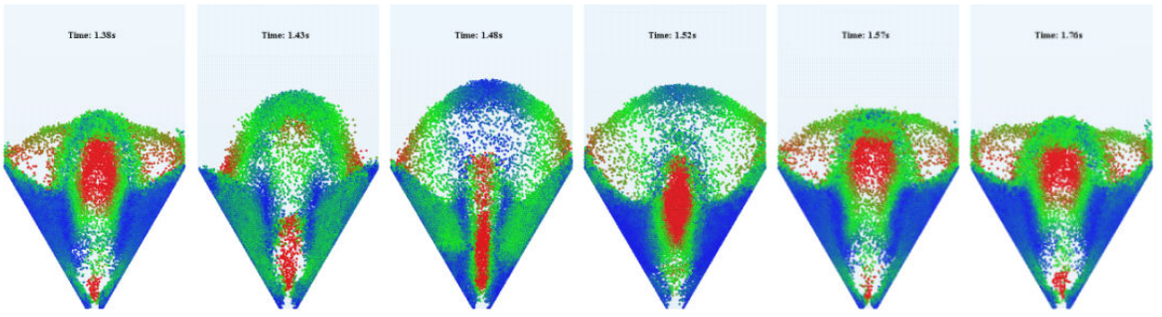

Figure 16. The periodical change of particle movement in the spout process(Red: high particle velocity; Blue: low particle velocity)

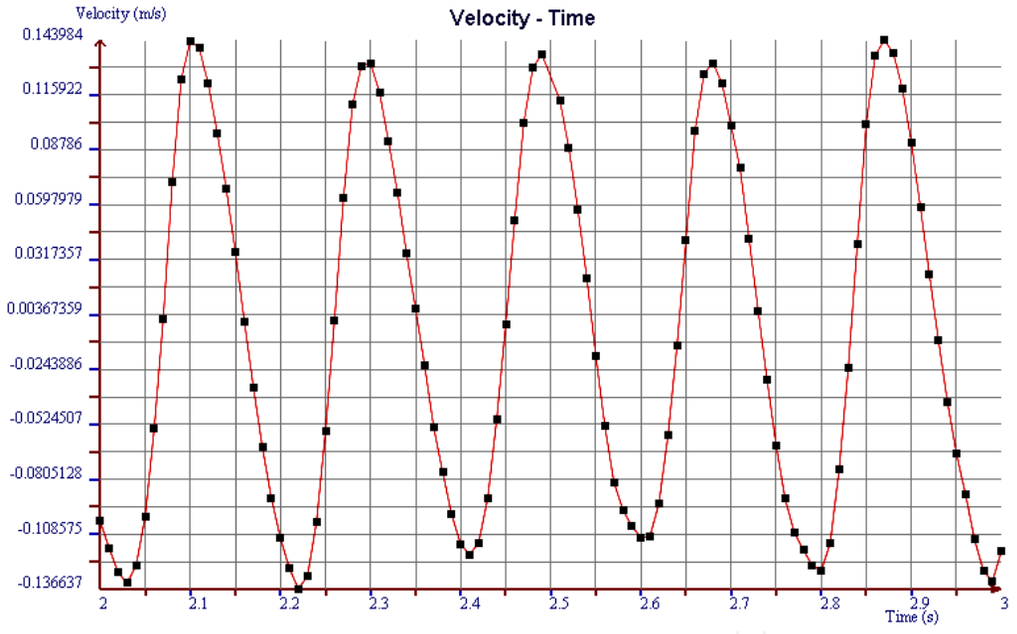

Figure 17. The periodical change of average particle vertical velocity in the spout process

The Discrete Element Method (DEM), which can resolve particle flow behaviors at an individual particle level, has been widely used for studying granular-fluid flow in fluidized-bed. The k–ε turbulence model, coupling with the DEM was used to simulate the particle spout behaviours in the coating process. The typical simualtion results in the conventional spouted bed are given in Fig.16 and Fig. 17. The simulation results indicate very rapid motion of the particles within the spout, with typical velocity of nearly 1 m/s. The oscillation cycle period of

particle clusters (T_c) can also be obtained as 190ms (1.38s -1.57s is one period and 1.57s-1.76s is one period in Fig. 16). The periodical change of average particle vertical velocity in the spout process in Fig. 17 can also validate that the oscillation cycle period of particle clusters is 190ms.

The single particle cycle time(T_p) is an important factor in the coating process, which can also be obained form the simulation results of the particle movement trajectory, as shown in Fig. 18. It can be found that the cycle index is 5 from 1s to 5s, so the cycle time can be obtained as 4.0s/5=0.8s. It can also be found that the time period of particle in spout area (the movement trajectory is indicated as red color) in one particle cycle time(T_s) is 40 ms, which is very short comparing with the single particle cycle time(T_p). It means that in the whole coating process, the growth time of the coating layer occupies only 5%(=40ms/800ms) of the total time of the coated process. The conventional spouted bed should be improved to obtain a high gas-solid contact efficiency.

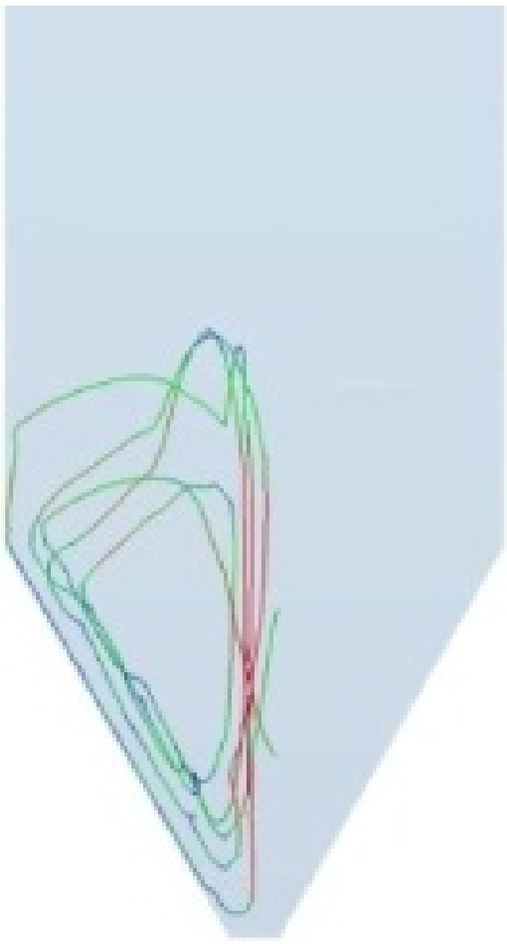

Figure 18. The particle movement trajectory in the spout process(1s-5s)

To sum up, the DEM-CFD simulation results can give the particle movement behaviors in details (T_c=190ms, T_p=800ms, T_s=40ms), so it has great potential in optimizing and scaling up the particle coating technology. It is obvious that the expansion of the spout area and reduction

of the cycle time will increase the coating efficiency and improve the performance of the coating layer. These methods should be considered as the basic principles of optimization and scale up of the coating technology.

- Euler-Euler simulation

To enhance the gas solid contact efficiency, the hydrodynamics of a three-dimensional conical spouted bed was studied using an Eulerian-Eulerian two-fluid model (TFM) incorporating the kinetic theory of granular flows. Four designs with traditional single-nozzle inlet, modified single-nozzle inlet, multi-nozzle inlet and swirl flow design inlet, as shown in Fig. 19, were simulated and compared.

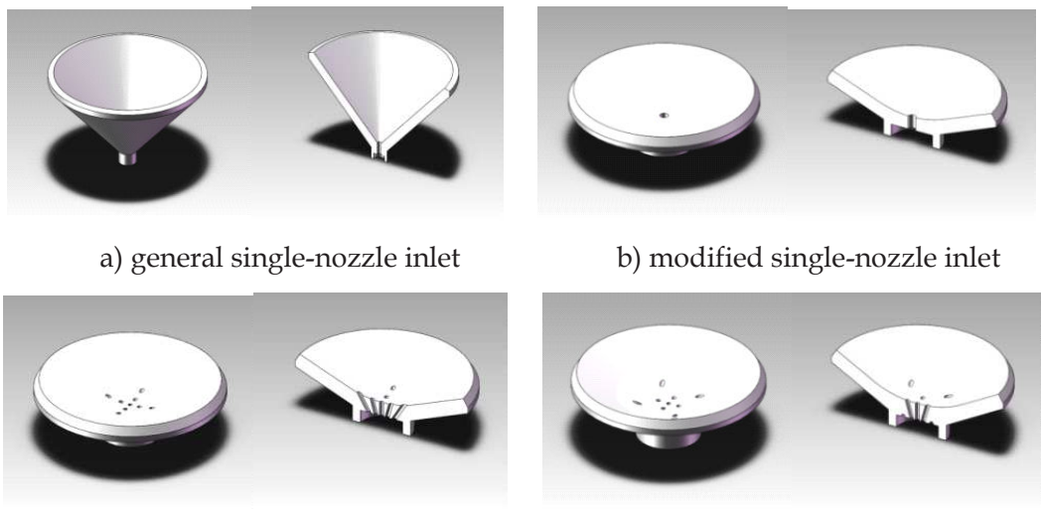

a) general single-nozzle inlet b) modified single-nozzle inlet

c) multi-nozzle inlet d) swirl flow design inlet

Figure 19. The pictures of different inlet designs

The typical simulation results are given in Fig. 20. The spout area is increased significantly with the multi-nozzle inlet. It can be found that the accumulation of particles near the wall disappears with a swirl flow design inlet, expecially at the bottom of the coater. These results illustrate that the design of the inlet is helpful to reduce the particle aggregation close to the wall and the spout area is enlarged as a result. The particle entrainment in the spouted bed with swirl flow design inlet increases significantly and the maximum spouted height is decreased at the same superficial gas velocity (0.6m/s), so T_s will be increased and the gas-solid contacting efficiency will be enhanced as a result.

To sum up, the swirl flow designed multi-nozzle gas inlet is better than any other gas inlets for obtaining a more uniform fluidization, which can disperse the gas to increase the gas-particle contact efficiency. In the future, the coating experimental results should be given to validate the good performance of this newly designed inlet with swirl flow multi-hole.

It should be indicated that the necessity of simulation for this process is obvious [15]. The new design and the details of particle movement can be obtained before experiments, so a lot of

time and money can be saved in the research process, and the results can be used as the targeted initial conditions for further optimization in experiments. On the other hand, how to obtain accurate and meaningful simulation results is very important, it is based on the basical studies of mathematical models and numerical simulation method.

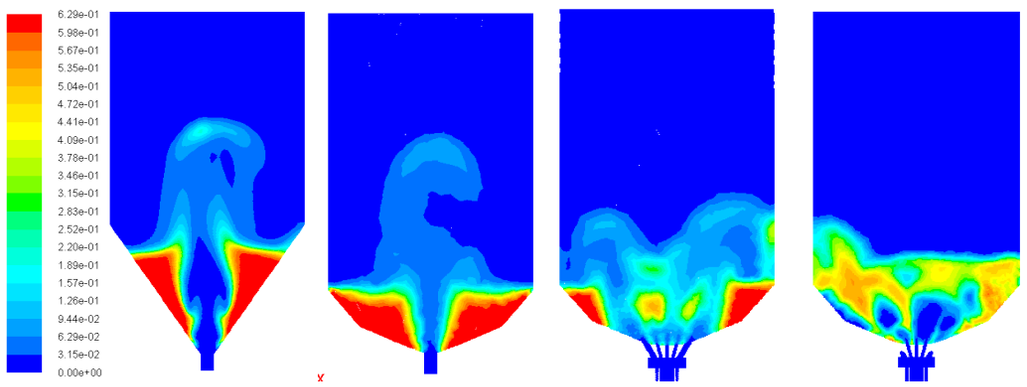

Figure 20. Profiles of the solid holdup under different inlet designs in the spouted bed at the same superficial gas velocity (0.6m/s)

3.3. Macroscale study

The macroscale study mainly focused on the process engineering analysis on the whole coating system, such as the pressure fluctuation analysis in the coating process [16, 17]. An example we have completed is the associated research between a reactor-scale pressure changes and coating process [18]. In this research, I have proposed a relationship about the change of pressure drop and the change of particle properties before and after the coating process of each layer. A convenient method for real-time monitoring the fluidized state of the particles in a high-temperature coating process is proposed based on this relationship. It will descibed in details as follows.

The conical spouted bed coating furnace is the main part of the coating system, which was designed carefully in experiments. Operations in particle spouting are sensitive to the geometry of the equipment and particle diameter/density. The following geometric parameters for stable operations in spouting bed are important, as shown in Fig. 21: (1) Cone included angle (γ), (2) Inlet diameter (D_o), (3) Column diameter (D_c), (4) Height of conical part (H_c). The pressure drop can be related to this parameters. There are also some parameters related to the particle properties, such as particle diameter d_p, static bed height H_o, particle density ρ_p, which are also very important to determinate the spouted bed hydrodynamics. The pressure drop changed with the superficial gas velocity and different stages are illustrated in Fig. 22 in details. The stable spouting state is the optimum state to achieve the efficient and uniform contact of particles with the reactive gas phase, Therefore, particles should remain the stable spouting state in the conical spouted bed coating furnace and ΔP_s is expected to be found during the whole coating process.

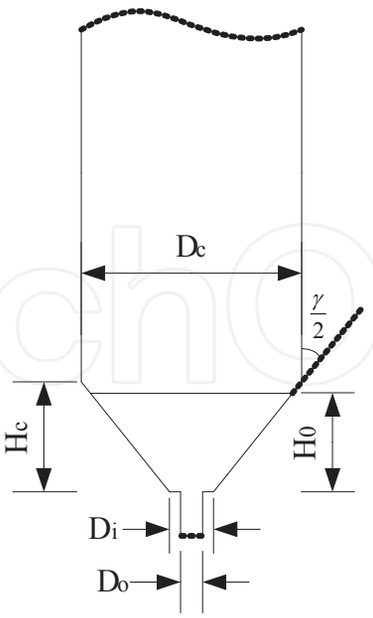

Figure 21. The geometric factors of the spouted bed using in the coating process

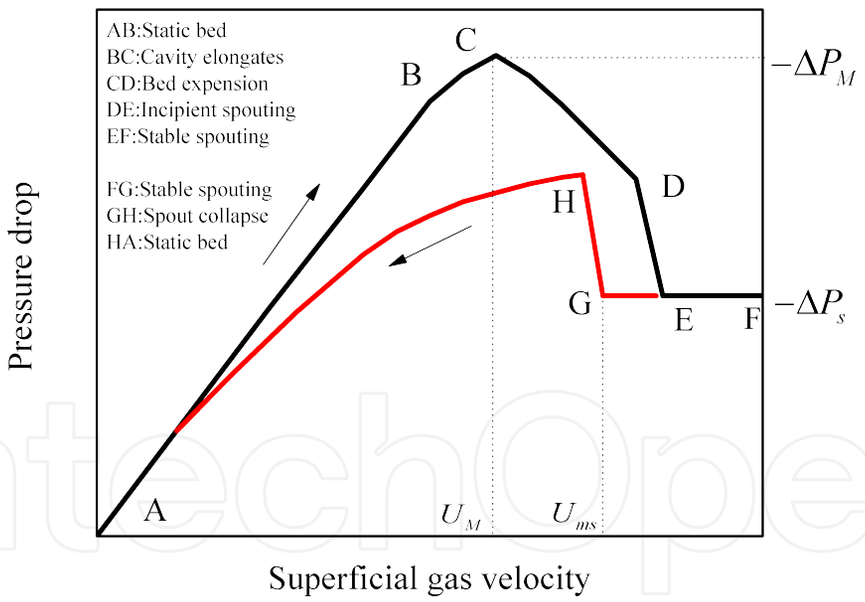

Figure 22. Pressure drop change in spouted bed with different superficial gas velocity

All the particles and graphite column tube are in the glowing red state at 1200-1600ºC. So it is unfeasible to obtain the pressure signals in the gas solid flow in the high temperature graphite column tube directly. But it is easy to measure the pressure signals at both ends of the coating furnace in the real coating process, for example points A&B are selected for measuring the pressure signals in our experiments as shown in Fig. 2. In this way, one can not know the pressure drop resulting of particle spouting accurately, because the pressure drop between points A&B

also includes pressure drops produced by the additional unit components, such as the nozzle, the insulation panel, the gas buffer device and others. Pressure drops in these specially designed graphite devices are often very large and can not be ignored, so the pressure drop resulting of particle spouting can not be obtained accurately, but the change of pressure drop values at points A&B at different coating time can be calculated from experimental results.

The pressure changes at points A&B in the coating process of four layers are given in Fig 23. It can be found that the pressure change is different in the coating process of four layers at points A&B. Point B is close to the outlet of the furnace, so the gage pressure at point B is almost not changed and nearly zero. The gage pressure at point A is changed distinctly during the coating process. Period a-b is the rising temperature process. Only argon is used as the fluidization gas. The flow rate is 362 L/min. The pressure at point A is increasing with the temperature. Period b-c is the buffer PyC coating process. In this coating process acetylene is introduced into the spouted bed as reactive gas. Similarly, Period d-e, f-g, h-i is the IPyC, SiC, OPyC coating process respectively. Period c-d, e-f, g-h is the process of adjusting the temperature. Besides, the fluidization gas changes to hydrogen at point f and changes back to argon at point g. The flow rate of argon remains 362 L/min in the whole process except the period f-g, and the temperature at point b and c is the same, so the change of the gage pressure drop ΔP from b to c represents the change of particle properties caused by buffer PyC coated layer. Similarly, the changes of ΔP from d to e, f to g, h to i represent the change of particle properties caused by IPyC, SiC, OPyC coated layer respectively. Period i-j is cooling process after the completion of coating experiments. The pressure at point B is not changed, so the change of pressure drop ΔP from h to i is equal to the change of pressure at point A from h to i. The change of pressure drop ΔP from h to i can be read as 580 Pa from the inset in Fig. 24. In the same way, It can be obtained that the changes of pressure drop ΔP from b to c, d to e, f to g are 367, 412, 705 Pa respectively from experimental results.

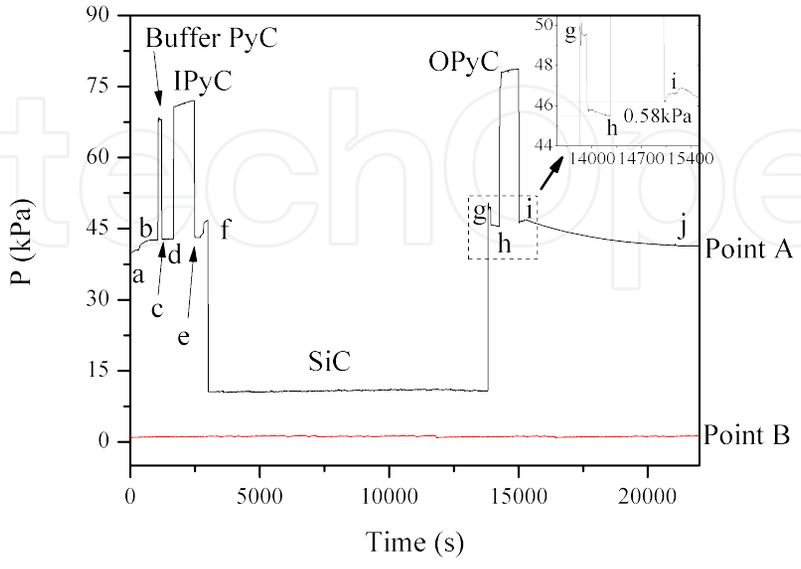

Figure 23. Pressure signals at points A&B during the successive coating process

The minimum spouting velocity can be related with the parameters of the spouted bed geometry and particle properties. Many researchers have given relationships about the minimum spouting velocity in different experiment conditions [19, 20], such as the D. Sathiyamoorthy's equation [21]. It has been indicated that the temperature only influence the constant coefficient and the index number is not changed with temperature. The experiments have been performed in the cold mockup of our spouted bed coating furnace and the following equations are proposed analogy with the literature reports:

$$U_{ms} = k_1 H_0^{1.499} \left(\rho_p - \rho_f\right)^{0.477} d_p^{0.610} \tag{1}$$

The constant k_1 is combination factor of the spouted bed geometrical parameters D_0, D_c, γ fluid density ρ_f and temperature. The pressure drop at stable spouting state ΔP_s can be related to the spouted bed geometry and particle properties, which expressed as follows:

$$\frac{-\Delta P_s}{H_0 \rho_b g} = 1.20 \left(\frac{H_0}{D_0}\right)^{0.08} \left(\mathrm{tg}\frac{\gamma}{2}\right)^{-0.11} \left(\frac{D_0 U_{ms} \rho_f}{\mu}\right)^{-0.06} \tag{2}$$

It can be found that the pressure drop at stable spouting state ΔP_s is a function of the spouted bed geometrical parameters and particle parameters. By substituting Eq.(1) into Eq.(2), considering that the gas density is small, and can be neglected compared to the solid density, then a simplified relationship can be obtained as:

$$-\Delta P_s = k \rho_b H_0^{0.99006} \rho_p^{-0.02862} d_p^{-0.0366} \tag{3}$$

The constant k is a combination factor and is not changed in the same spouted bed under the same temperature, so k is not changed before and after the coating process of each layer. The change of pressure drop can be deduced from Eq.(3). The time points 1 and 2 are represent of the time points before and after the coating process of each layer. Then the simplified form of the pressure drop can be obtained as

$$\frac{-\Delta P_{s1} - \left(-\Delta P_{s2}\right)}{\varphi_1 - \varphi_2} = k, \text{ in which } \varphi = \rho_b H_0^{0.99006} \rho_p^{-0.02862} d_p^{-0.0366} \tag{4}$$

It can be found that, if only particle properties change, for example, in the coating process of particles, the change of pressure drop is linear with the change of combination factor φ about particle density, particle bulk density and static bed height. The change of particle density ρ_p and diameter d_p during the coating process can be calculated, as shown in Fig. 24. Then the bed density ρ_b and static bed height H_0 can be obtained according to the experimental bulk

coefficient and the spouted bed geometrical parameters (D_c=150 mm), as shown in Fig. 25. The change of combination factor $\Delta\varphi$ during coating process of buffer PyC, IPyC, SiC, OPyC can be obtained as 28.06, 31.70, 55.83, 45.63 by Eq.(4). The change of pressure drop $\Delta(\Delta P)$ during coating process of buffer PyC, IPyC, SiC, OPyC layer has been obtained as 367, 412, 705, 580 Pa respectively from Fig. 23, k can be calculated as 13.08, 12.99, 12.63, 12.71 in four coating process of buffer PyC, IPyC, SiC, OPyC layer. It can be found that k is almost a constant as shown in Fig. 26. The consistent relationship Eq.(4) is verified by experimental results.

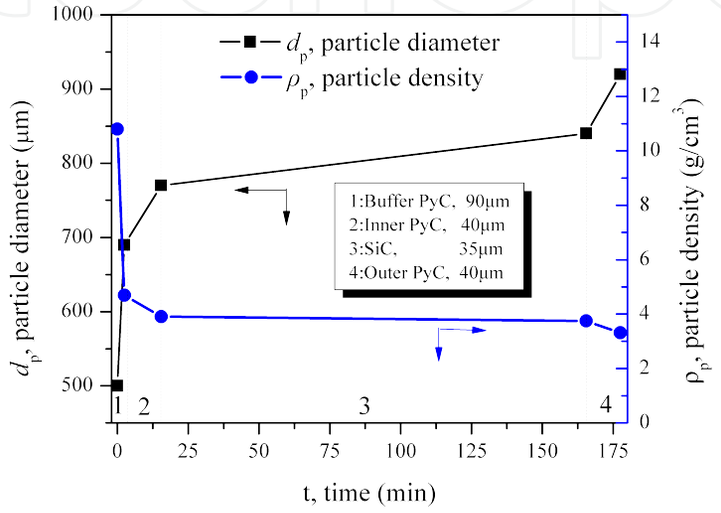

Figure 24. The change in particle diameter and particle density during successive (TRISO) coating on UO_2 micro-spheres

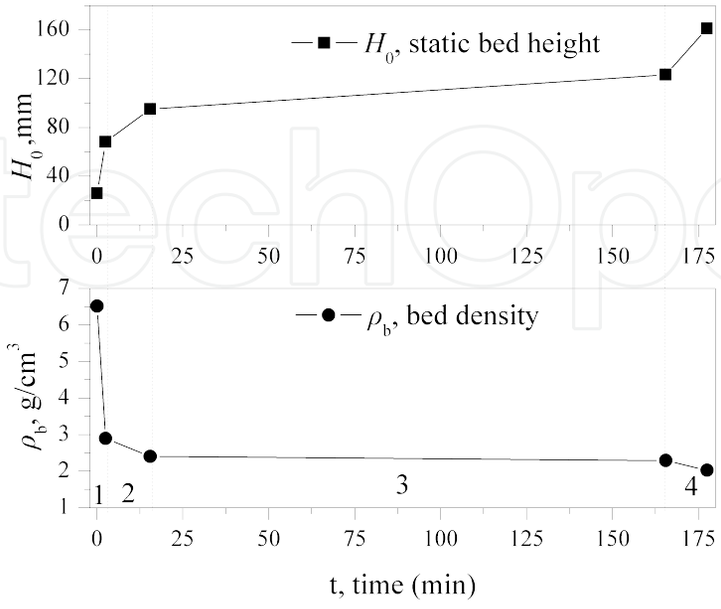

Figure 25. The change in static bed height and bed density during successive (TRISO) coating on UO_2 micro-spheres

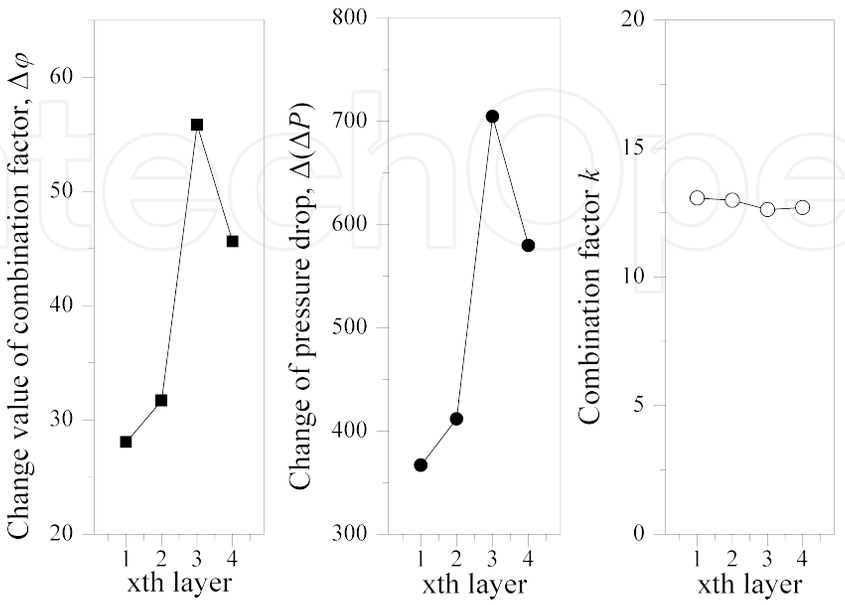

Figure 26. The change of pressure drop, the change of combination factor φ and combination factor k during successive (TRISO) coating on UO_2 micro-spheres

Through the above process, a convenient method for on-line monitoring the fluidized state of the particles in a high-temperature coating process can be proposed. The pressure drop change before and after coating can be used effectively as real-time analysis of particle flow conditions. The combination factor φ can be calculated on the basis of design values of coating layer, the pressure drop change can be obtained from the experimental results, so k can be calculated in four coating process, then a constant k should be obtained. One can compare k values to estimate the fluidization state at different coating process of four coating layers. If an abnormal value is found, which indicates the poor quality of particle fluidization state during the coating process, and then the quality of the coated layer will be affected. Additionally, k can also be estimated firstly by a series of experiments, the pressure drop changes can be calculated by Eq.(4) in the same spouted bed coating furnace according to the design value of the coated layer, and then real-time comparative analysis with the experimental results of pressure drop changes can be performed to monitor the fluidized state of the particles on-line in the coater.

4. Brief summary

The multiscale study of the coating technology of nuclear fuel kernels are discussed above, and the brief summary can be given as follows:

1. In microscale study, it was found that the droplet deposition mechanism can be used to explain the formation of the PyC layer in the fuel particle coating process. The nano-spherical carbon particle is generated at first, and then deposit on the surface of fuel particle. The pure β-SiC can be prepared in the experimental temperature range from 1520-1600ºC. The density change of the SiC coated layer is mainly due to the micropores in the coated layer, not the doped C, Si and other impurities. The oxidization of SiC coating layer was not obvious below 1 200 ºC. The oxidization of SiC coating layer was significant gradually from 1 400 ºC, but the oxidation rate is very slow.
2. In mesoscale study, some key parameters in coating process are proposed, such as single particle cycle time and so on, which can be obtained exactly from DEM-CFD simulation results. The newly proposed gas inlet with swirl flow designed multi-nozzle is better than any other gas inlets for obtaining a more uniform fluidization, which can disperse the gas to increase the gas-particle contact efficiency.
3. In macroscale study, the pressure signals of the coater during the coating process of real TRISO UO_2-coated particles are given and analyzed. A relationship about the change of pressure drop and the change of particle properties before and after the coating process of each layer is proposed. This relationship is also validated by the experimental results. A convenient method for real-time monitoring the fluidized state of the particles in a high-temperature coating process is proposed based on the proposed relationship.

5. Conclusions and prospective

In this chapter, the multiscale study concept of the coating technology is stated and validated as an effective and necessary method to develop the coating technology of nuclear fuel kernels from the lab to the factory. It should be indicated that the application of the coating technology for other usages rather than nuclear industry is extensive, such as CNT preparation and suface modification of catalyst particles. The multiscale study of the coating technology can be seen as a universal methodology in the R&D of the coating process, especially in the field of fluidized bed chemical vapor deposition (FB-CVD).

The FB-CVD method is a suitable technique for preparing various kinds of films/layers on the spherical materials by initiating chemical reaction in a gas. This technique can be used for many purposes, such as synthesizing carbon nanotube composite photocatalyst ((CNT)/Fe-Ni/TiO_2). Also, some modified method based on FB-CVD, such as plasma-enhanced FB-CVD, has been used to prepare the transparent water-repellent thin films on glass beads in modern surface engineering treatment. So the investigation of FB-CVD method is helpful and important for modern surface treatments.

This multiscale study should be developed in the future, especially in the the mutual coupling reasearch in micro-, meso- and micro- scales, such as the effect of fluidized state on the homogeneity and compactness of coating materials. Also, this method should play an important role in the study of the scale-up methodology in the field of FB-CVD.

Appendix

γ	Cone included angle
D_o	Inlet diameter, m
D_i	Diameter of the bed bottom, m
D_c	Column diameter, m
H_c	Height of conical part, m
H_o	Static bed height, m
d_p	Particle diameter, m
ρ_p	Particle density, kg/m^3
ρ_f	Fluid density, kg/m^3
ρ_b	Bed density, kg/m^3
ΔP_M	Maximum pressure drop, Pa
ΔP_s	Pressure drop at the stable spouting state, Pa
U_M	Spouting velocity at maximum pressure drop, m/s
U_{ms}	Minimum spouting velocity at the stable spouting state, m/s
g	Gravity, m/s^2
V_p	The volume of spout area, m^3
T_c	The oscillation cycle period of particle clusters, s
T_p	The single particle cycle time, s
T_s	The time period of particle in spout area in a particle cycle time, s

Acknowledgements

The author would like to thank the National S&T Major Project (Grant No. ZX06901), the Independent Research Projects of Tsinghua University (20111080971) and Research Fund for the Doctoral Program of Higher Education of China(20121010010) for the financial support provided. Also, thanks go to Bing Liu, Youlin Shao, Jing Wang, Junguo Zhu, Bing Yang, Bingzhong Zhang, as my best colleagues. All the results of this chapter are completed together with them. The author himself is responsible for all of the errors of this chapter.

Author details

Malin Liu*

Address all correspondence to: liumalin@tsinghua.edu.cn

Institute of Nuclear and New Energy Technology, Tsinghua Univerisity, Beijing, China

References

[1] Lee Y-W, Park J-Y, Kim YK, Jeong KC, Kim WK, Kim BG, et al. Development of HTGR-coated particle fuel technology in Korea. Nuclear Engineering and Design. 2008; 238(11): 2842-2853.

[2] Nickel H, Nabielek H, Pott G, Mehner AW. Long time experience with the development of HTR fuel elements in Germany. Nuclear Engineering and Design. 2002; 217(1-2): 141-151.

[3] Sawa K, Ueta S. Research and development on HTGR fuel in the HTTR project. Nuclear Engineering and Design. 2004; 233(1-3): 163-172.

[4] Tang C, Tang Y, Zhu J, Zou Y, Li J, Ni X. Design and manufacture of the fuel element for the 10 MW high temperature gas-cooled reactor. Nuclear Engineering and Design. 2002; 218(1-3): 91-102.

[5] Barnes CM, Marshall DW, Keeley JT, Hunn JD. Results of Tests to Demonstrate a 6-in.-Diameter Coater for Production of TRISO-Coated Particles for Advanced Gas Reactor Experiments. Journal of Engineering for Gas Turbines and Power. 2009; 131(5): 052905.

[6] Reznik B, Gerthsen D, Zhang WG, Huttinger KJ. Microstructure of SiC deposited from methyltrichlorosilane. Journal of the European Ceramic Society. 2003; 23(9): 1499-1508.

[7] Hélary D. , Bourrat X., Dugne O. , Maveyraud G. , Pérez M., P. G. Microstructures of Silicon Carbide and Pyrocarbon Coatings for Fuel Particles for High Temperature Reactors. Proceedings of 2nd International Topical Meeting on HTR Technology. 2004.

[8] Lopez-Honorato E, Tan J, Meadows PJ, Marsh G, Xiao P. TRISO coated fuel particles with enhanced SiC properties. Journal of Nuclear Materials. 2009; 392(2): 219-224.

[9] Liu M, Liu B, Shao Y. The study on pyrolytic carbon powder in the coating process of fuel particle for high-temperature gas-cooled reactor. ICONE18-30137, Volume 1: 545-549. 2010.

[10] Fang C, Liu M-L. The study of the Raman spectra of SiC layers in TRISO particles. Acta Physica Sinica. 2012; 61(9): 097802.

[11] Liu M, Liu B, Shao Y. Study on Properties of SiC Coated Layer for HTGR Fuel Particles (in chinese). Atomic Energy Science and Technology. 2012a; 46(09): 1087-1092.

[12] Lopez-Honorato E, Meadows PJ, Xiao P, Marsh G, Abram TJ. Structure and mechanical properties of pyrolytic carbon produced by fluidized bed chemical vapor deposition. Nuclear Engineering and Design. 2008; 238(11): 3121-3128.

[13] Rohmfeld S, Hundhausen M, Ley L. Raman scattering in polycrystalline 3C-SiC: Influence of stacking faults. Physical Review B. 1998; 58(15): 9858-62.

[14] Liu M, Liu B, Shao Y. Optimization of the UO2 kernel coating process by 2D simulation of spouted bed dynamics in the coater. Nuclear Engineering and Design. 2012b; 251: 124-130.

[15] Duarte CR, Olazar M, Murata VV, Barrozo MAS. Numerical simulation and experimental study of fluid-particle flows in a spouted bed. Powder Technology. 2009; 188(3): 195-205.

[16] Lopes NEC, Moris VAS, Taranto OP. Analysis of spouted bed pressure fluctuations during particle coating. Chemical Engineering and Processing. 2009; 48(6): 1129-1134.

[17] Xu JA, Bao XJ, Wei WS, Shi G, Shen SK, Bi HT, et al. Statistical and frequency analysis of pressure fluctuations in spouted beds. Powder Technology. 2004; 140(1-2): 141-154.

[18] Liu M, Shao Y, Liu B. Pressure analysis in the fabrication process of TRISO UO2-coated fuel particle. Nuclear Engineering and Design. 2012c; 250: 277-283.

[19] Zhong WQ, Chen XP, Zhang MY. Hydrodynamic characteristics of spout-fluid bed: Pressure drop and minimum spouting/spout-fluidizing velocity. Chemical Engineering Journal. 2006; 118(1-2): 37-46.

[20] Zhou J, Bruns DD, Finney CEA, Daw CS, Pannala S, Mccollum DL. Hydrodynamic Correlations with Experimental Results from Cold Mockup Spouted Beds for Nuclear Fuel Particle Coating. AIChE Annual Meeting. 2005.

[21] Sathiyamoorthy D, Rao VG, Rao PT, Mollick PK. Development of pyrolytic carbon coated zirconia pebbles in a high temperature spouted bed. Indian Journal of Engineering and Materials Sciences. 2007; 17(5): 349-52.